Impact parameter dependence of hard photon production in intermediate energy heavy-ion collisions

Martinez, G; Diaz, J; Franke, M; Hlavac, S; Holzmann, R; Lautridou, P; Lefevre, F; Löhner, H; Marin, A; Marques, M

Impact parameter dependence of hard photon production in intermediate energy heavy-ion collisions [✩]

G. Martínez [a], J. Díaz [a], M. Franke [b], S. Hlaváč [c,1], R. Holzmann [c], P. Lautridou [d,2],
F. Lefèvre [d,3], H. Löhner [e], A. Marín [a], M. Marqués [d,4], T. Matulewicz [d,5], W. Mittig [d],
R.W. Ostendorf [d,6], J.H.G. van Pol [e], J. Québert [f], P. Roussel-Chomaz [d], Y. Schutz [d],
A. Schubert [c], R.H. Siemssen [e], R.S. Simon [c], Z. Sujkowski [g],
V. Wagner [h], H.W. Wilschut [e]

[a] *Instituto de Física Corpuscular (CSIC-Universidad de Valencia) and Departamento de Física Atómica, Molecular y Nuclear, 46100 Burjassot, Spain*
[b] *II Physikalisches Institut Universität Gießen, D-35392 Gießen, Germany*
[c] *Gesellschaft für Schwerionenforschung, D-64291 Darmstadt, Germany*
[d] *Grand Accélérateur National d'Ions Lourds, BP 5027, 14021 Caen, France*
[e] *Kernfysisch Versneller Instituut, 9747 AA Groningen, The Netherlands*
[f] *Centre d'Etudes Nucléaires de Bordeaux-Gradignan, 33175 Gradignan, France*
[g] *Soltan Institute for Nuclear Studies, 05-400 Swierk, Poland*
[h] *Nuclear Physics Institute, 250 68 Řež, Czech Republic*

Abstract

Hard photon production was investigated in the system $^{86}Kr + ^{nat}Ni$ at 60 A MeV for a wide range of impact parameters. The parameters characteristic of hard photon emission such as source velocities, angular distributions and energy spectra were studied from peripheral to central collisions. The energy spectrum is seen to be strongly dependent on the centrality of the collision reflecting both a static and dynamic momentum distribution of the nucleons inside the collision zone.

Since the first measurements of hard photons by Beard et al. [1] and Grosse et al. [2] a large amount of data have been collected on the production of hard photons in inclusive heavy-ion collisions. These cover a wide range of target–projectile combinations and energies between 15 and 124 MeV/u. From the systematics [3] it was deduced that the hard photons mainly originate from the incoherent superposition of bremsstrahlung radiation emitted during individual first chance neutron–proton collisions within the participant zone. A few experiments since have investigated the

dependence of the hard photon production mechanism on the impact parameter which was selected by either the charged particle multiplicity [4,5] or the mass of the projectile like fragments (PLF) [6,7]. A strong variation of the photon multiplicity was observed with the largest multiplicity for the most central collisions as suggested by the n–p bremsstrahlung model. Within this frame, Riess et al. [6] have used the photon multiplicity to determine impact parameter.

The exclusive measurements also demonstrated that the photon energy spectrum depends on the impact parameter, whereby softer spectra were observed for the more peripheral collisions. This dependence is consistent with the fact that the energy available in the N–N center-of-mass system for the production of a photon is provided by the beam velocity and the velocity due to the Fermi motion of the two nucleons, so at bombarding energies close to the Fermi energy (≈ 40 MeV) the hardness of the energy spectrum reflects the momentum distribution of the nucleons within the collision zone. It should be noted, however, that for the central collisions studied so far [4,5] the charged particle multiplicity could only be used qualitatively to identify non-peripheral reactions.

In this paper we report on an investigation of hard photon production with an improved identification of peripheral and central reaction channels, and therefore with a better impact parameter selection. We find that the photon spectrum changes appreciably with the impact parameter. By comparing with theoretical models we conclude that the shape of the photon spectrum depends not only on the intrinsic momentum distribution but also on the dynamics of the reaction.

The data were taken for the ^{86}Kr + ^{nat}Ni reaction at 60 A MeV with a ^{86}Kr beam delivered by the GANIL accelerators with an average intensity of 12 enA. The total accumulated beam was 8.1×10^{14} particles. The nickel target was 11.89 mg/cm^2 thick. Peripheral reactions were selected by the masses of the PLF's which were detected and identified with a Z and A resolution of 0.4 and 0.8 units FWHM, respectively, with the energy-loss magnetic spectrometer SPEG [8] placed at 0°. The angular range covered by SPEG in the horizontal plane was between $-0.4°$ and $+0.4°$ and the momentum acceptance ($\Delta p/p$) was 7%. For central collisions use was made of the multiplicity of the charged particles detected in the KVI hodoscope [9] consisting of 60 phoswich detectors positioned in the

vacuum chamber in front of the spectrometer and covering an angular range in the laboratory system between 3.5° and 23.0°.

The angular distributions and energy spectra for photons were measured with the TAPS photon spectrometer [10] consisting of 5 square blocks of 64 hexagonal BaF$_2$ detectors each, positioned around the target at an average distance of 62 cm. The array covered a solid angle of $\sim 17\%$ of 4π, spanning in the laboratory system a nearly continuous angular range between 35° and 165°. For the tagging of charged particles each BaF$_2$ detector was equipped with a plastic detector (CPV) in front of it. Neutrons and the remaining charged particles were rejected by their characteristic pulse shape in the BaF$_2$ and their time-of-flight with an ultimate time resolution of 600 ps including the spread of 550 ps in the time structure of the beam bursts. Any remaining contamination of the photon events due to improperly identified hadrons was negligible. Cosmic-ray induced events were identified and rejected with a trace recognition algorithm. Before and after the experiment the BaF$_2$ detectors were calibrated using γ-ray sources with energies up to 4.4 MeV and the 38.5 MeV mean energy deposited by minimum-ionizing cosmic-ray muons. The cosmic-ray events were recorded during the experiment (including beam-off periods) and served as a gain monitor. From the π^0 measured invariant mass distribution we have estimated that for 50 MeV photons the final energy resolution ($\Delta E/E$) was 5% and the angular resolution ($\Delta\theta$) 1°.

The inclusive photon production was analyzed assuming an exponential energy spectrum characterized by the inverse slope parameter E_0 and the angular distribution to be isotropic with a dipolar contribution characterized by the parameter α. The photon emission was assumed to take place in a rest frame moving at velocity β_S. The double differential cross section thus has the following form in the laboratory frame [4]:

$$\frac{\mathrm{d}^2\sigma}{\mathrm{d}E\,\mathrm{d}\Omega} = \frac{K}{Z}\left(1 - \alpha + \alpha\,\frac{\sin^2\theta}{Z^2}\right)\exp\left(-\frac{ZE}{E_0}\right), \qquad (1)$$

with

$$Z = \gamma_S(1 - \beta_S\cos\theta)\ .$$

The fit of expression (1) to our data has been performed for photons with energies larger than 30 MeV. The results are summarized in Table 1. The slope parameter

Table 1
Parameters characterizing the inclusive hard photon ($E_\gamma \geqslant 30$ MeV) production in the reaction ^{86}Kr + ^{nat}Ni at 60 MeV/u assuming an exponential energy spectrum and an isotropic + dipolar angular distribution for a moving source

K (μb sr^{-1} MeV^{-1})	σ_γ (mb)	P_γ ($\times 10^{-4}$)	α	E_0 (MeV)	β_S
71(4)	3 6(0 2)	1.20(0.03)	0 15(0 06)	19.4(0 4)	0 176(0.007)

The slope parameter E_0 has been corrected for the detector response.

E_0 has been corrected for the detector response. The photon source velocity, $\beta_S = 0.176 \pm 0.007$, is compatible with the velocity of the N–N center-of-mass, $\beta_{NN} = 0.177$. Neutral pions were identified by means of the γ–γ invariant mass, with a resolution of 13% FWHM. From the π^0 production we deduce that the contribution to hard photon production of single photons stemming from π^0 decay was only 1.3% of the total yield. The measured photon cross section, $\sigma_\gamma = 3.6 \pm 0.2$ mb, is in general agreement with the scaling law on the photon production excitation function [3]. The inclusive probability to produce a photon with energy larger than 30 MeV per neutron–proton collision, P_γ^{incl}, is given by

$$M_\gamma^{incl} \equiv \frac{\sigma_\gamma}{\sigma_R} = \langle N_{pn}\rangle P_\gamma^{incl}$$

$$= \langle N_{pn}\rangle P_0 \exp(-30/E_0^{incl}), \qquad (2)$$

where $\sigma_R = 4.4$ b is the geometrical reaction cross section and $\langle N_{pn}\rangle = 7.0$ the number of proton–neutron participants averaged over the impact parameter and calculated using the geometrical model of Ref. [11].

The exclusive photon data were analyzed as a function of the charged particle multiplicity, M_{CP}, measured in the hodoscope and as a function of the mass of the projectile fragment, A_{PLF}. Fig. 1 shows the measured photons multiplicity, as a function of M_{CP} and A_{PLF}.

Considering Eq. (2) one can calculate for a given multiplicity, M_γ^{excl}, the number of participants, as suggested in Ref. [6],

$$N_{pn}(b) = \frac{M_\gamma^{excl}}{P_\gamma^{excl}}, \qquad (3)$$

where P_γ^{excl} is parametrized by

$$P_\gamma^{excl} = P_0 \exp(-30/E_0^{excl}), \qquad (4)$$

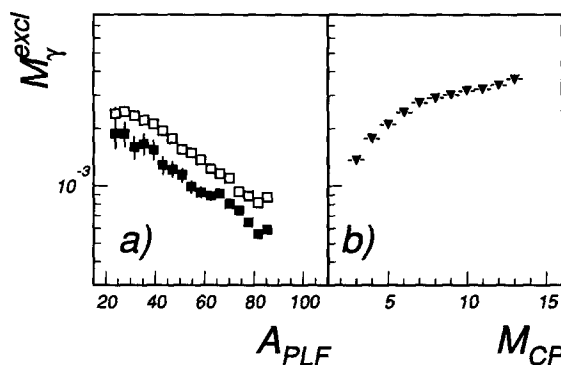and P_0 is deduced from the inclusive measurement according to Eq. (2). Using the geometrical model of

Fig. 1 Photon multiplicity spectra measured in the reaction ^{86}Kr + ^{nat}Ni at 60 MeV/u and plotted as a function of (a) the projectile-like fragment mass (open squares for SPEG rigidity at 85% $B\rho$ and closed squares for SPEG rigidity at 90% $B\rho$) and (b) the charged particle multiplicity

Ref. [6], the correspondence of the N_{pn} with impact parameter can be made.

However, rather than relying on this model we present our results as a function of M_γ^{excl}. For reference, the impact parameter scale given by Eq. (3) and Ref. [6] has been added in Figs. 1 and 2. As observed in the figures our reaction channel covers the full range of impact parameters in fine steps. With the horizontal
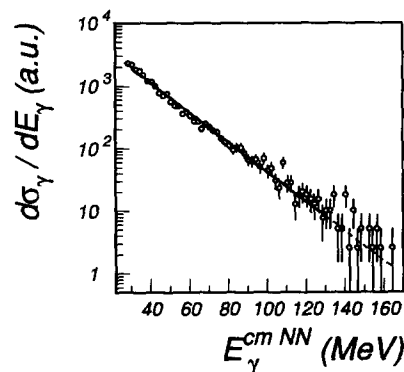

Fig 2. Hard photon energy spectrum calculated in the NN center of mass measured in the reaction ^{86}Kr + ^{nat}Ni at 60 MeV/u for $M_{CP} = 5$

"errors" bars the range of impact parameter in which a reaction channel occurs has been estimated from the abrasion–ablation model [12] for fragment production and FREESCO [13] for light charged particle production.

To study the evolution of the properties of the hard photon production we have constructed for each impact-parameter the angular distribution and the
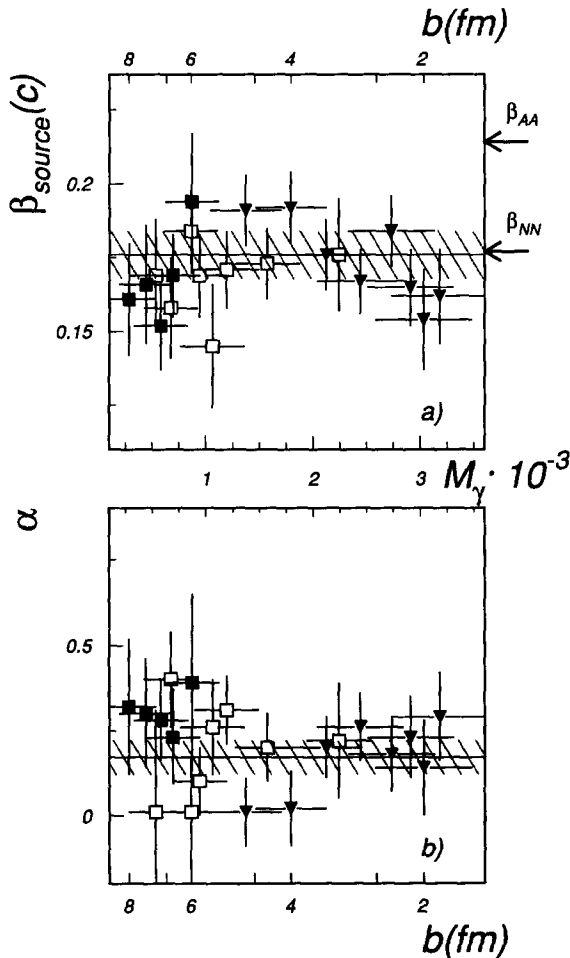

Fig 3 Hard photon source velocity (a) and anisotropy factor (b) as a function of the photon multiplicity measured in the reaction ^{86}Kr + ^{nat}Ni at 60 MeV/u The associated impact parameters are also indicated on the top and bottom scales of the figure The triangles indicate data selected with the charged particle multiplicity, the open squares (SPEG at 85% Bp) and closed squares (SPEG at 90% Bp) indicate data selected using the mass of the PLF The hatched area marks one standard deviation The horizontal error bars indicate the estimated resolution on the impact parameter

energy spectrum from the corresponding set of photon data. A typical energy spectrum measured in coincidence with $M_{CP} = 5$ is shown in Fig. 2. We have assumed that the gross properties of the photon production remain the same and have analyzed the data according to Eq. (1). The deduced values for the source velocity, β_S, and the anisotropy factor, α, are plotted in Figs. 3a and 3b respectively as a function of the photon multiplicity, i.e. the impact parameter. No systematic variation with the impact parameter is found and the source velocities are consistent with the nucleon–nucleon center-of-mass velocity within one standard deviation (hatched area). The anisotropy factor is also seen to be constant over the range of impact parameters probed. This result indicates that the mechanism of hard photon production via bremsstrahlung from individual first chance neutron–proton collisions does not change with the centrality of the collision. In particular there is no indication for either photon emission from a thermalysed region which would yield a velocity intermediate between β_{NN} and the velocity of the nucleus–nucleus center of mass, $\beta_{AA} = 0.22$. Our collaboration has found evidence for such a component in a more asymmetric system and at higher energies (^{36}Ar + ^{197}Au at 95 A MeV) [14].

The slope parameter, E_0, corrected for the detector response is plotted versus the photon multiplicity (impact parameter) in Fig. 4. One observes a strong decrease (27%) when one goes from central collisions to peripheral ones. This observation is in agreement with results reported earlier [4,5,15] where, however, because of the crude impact parameter selection, it was not possible to observe a detailed dependence. In our data we observe that the hardness of the photon spectrum decreases slowly from the most central collisions to 5–6 fm, that is as long as projectile and target overlap more than 50%. For larger impact parameters ($b > 5$–6 fm) the energy spectrum becomes rapidly softer (E_0 decreases) moving to peripheral collisions when the contribution from nucleons on the surface becomes predominant. Since in the neutron–proton bremsstrahlung model the photon energy spectrum reflects the momentum distribution of the nucleons within the participant zone, the observed change in the shape of the energy spectrum can result from two factors. The first one, which we call static, reflects the density distribution of the nucleons inside the nucleus which decreases when one moves from the interior to the surface of the
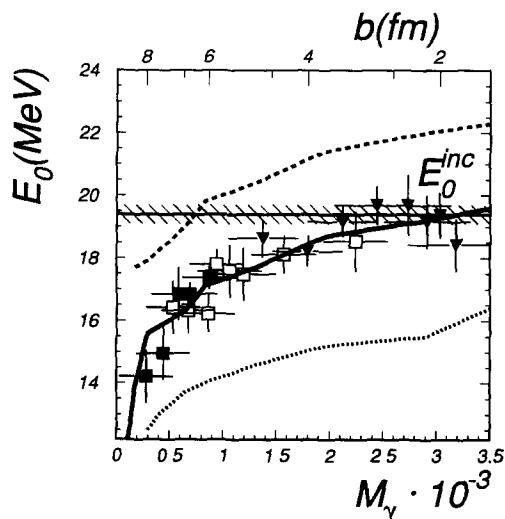
Fig. 4. Variation of the slope parameter of the hard photon spectra with photon multiplicity and impact parameter as measured in the reaction $^{86}Kr + ^{nat}Ni$ at 60 MeV/u Symbols are the same as in Fig 3 The horizontal error bars indicate the width of the impact parameter bin. The solid line is the result of a BUU calculation The dashed line is obtained from a BUU calculation by switching off the density variation in the nucleus and the dotted line is obtained by considering this density variation only.

nucleus. The second factor, the dynamic one, would be due to the dynamics of the collision on the momentum distribution of the nucleons inside the projectile–target overlap zone. The solid line in Fig. 4 shows the result of a BUU simulation [16] using the photon cross section parameterization of Ref. [17] for photons produced during the first 70 fm/c of the reaction. The calculation reproduces the observed behavior of E_0. To establish the origin of the observed E_0 dependence we have performed two more calculations. For the first one we have chosen as the initial momenta of the nucleons in the target and the projectile the Fermi momentum (1.36 fm^{-1}) instead of using the local density approximation. The result is shown by the dashed line in Fig. 4.

The second calculation assumes that all nucleons in the overlap zone collide once with the momentum distribution as in BUU at initialization, with the projectile nucleons boosted by the beam velocity. The results is shown as the dotted line in Fig. 4. One observes that only the dynamical calculation can reproduce the measured variation of the slope. Therefore the photon spectrum is also sensitive to the dynamical momentum distribution which is related to the compression at the beginning of the collision. If one also considers thermal photons [3] produced in a latter stage of the collision (up to 150 fm/c) E_0 is reduced by about 5%, which falls below the data. This observation confirms that photons from a thermalyzed region produced in the later stage of the collision do not contribute significantly.

In conclusion, we have investigated the properties of hard-photon production as a function of photon multiplicity (impact parameter). We have shown that almost the entire range of impact parameters can be selected in fine steps using the charged particle multiplicity measured in the forward direction and the mass and velocity of the projectile-like fragments. This technique is based on the strong correlation between these observables and the photon multiplicity which scales in the p–n bremsstrahlung model with impact parameter. We have then demonstrated that in the reaction $^{86}Kr + ^{nat}Ni$ at 60 A MeV the mechanism of hard-photon production does not change with the centrality of the collision.

Finally, we have shown that the more central reactions lead to harder photon spectra and that a significant variation in the slope parameter occurs at large impact parameters where the nucleus surface becomes the main participant in the collision. According to model calculations this effect reflects both the lower density on the surface of the nuclei and the higher densities reached during the reaction.

References

[1] K B. Beard et al., Phys. Rev C 32 (1985) 1111

[2] E. Grosse et al , Europhys Lett 2 (1986) 9.

[3] W. Cassing et al., Phys. Rep 188 (1990) 365;
H. Nifenecker and J A Pinston, Prog Part Nucl. Phys. 23 (1989) 271.

[4] M. Kwato et al., Nucl Phys A 489 (1988) 368

[5] L G Sobotka et al , Phys. Rev C 44 (1991) R2257, C 46 (1992) 819 (E);
T. Reposeur et al , Phys Lett. B 276 (1993) 418,
E Migneco et al , Phys. Lett B 298 (1993) 46

[6] S Riess et al., Phys Rev Lett 69 (1992) 1504.

[7] R. Hingmann et al., Phys. Rev Lett 58 (1987) 759

[8] L Bianchi et al , Nucl Instrum. Methods A 276 (1989) 509.

[9] H K W. Leegte et al., Nucl. Instrum. Methods A 313 (1992) 26, 33 (1993)

[10] R Novotny, IEEE Trans. Nucl. Sc 38-2 (1991) 379.

[11] H Nifenecker and J P Bondorf, Nucl. Phys A 442 (1985) 478.

[12] J.J Gaimard and K -H. Schmidt, Nucl. Phys A 531 (1991) 709

[13] G. Fai and J Randrup, Comput. Phys. Commun. 42 (1986) 385

[14] A. Schubert et al , Phys Rev. Lett 72 (1994) 1608.

[15] G Martínez et al , Nouvelles du GANIL 44 (1993) 43

[16] G. Wolf et al., Nucl Phys A 552 (1993) 559

[17] M. Schafer et al , Z Phys. A 339 (1991) 391.

[18] M Marqués, Nouvelles du GANIL 45 (1993) 45